BIOLOGY OF REPRODUCTION **79,** 1038–1045 (2008)
Published online before print 16 July 2008.
DOI 10.1095/biolreprod.108.069492

A Phenotypic Spectrum of Sexual Development in *Dax1* (*Nr0b1*)-Deficient Mice: Consequence of the C57BL/6J Strain on Sex Determination[1]

Susan Y. Park,[3,4] Eun-Jig Lee,[4] Donna Emge,[4] Carolyn L. Jahn,[5] and J. Larry Jameson[2,4]

Departments of Medicine[4] and Cell and Molecular Biology,[5] Division of Endocrinology, Metabolism, and Molecular Medicine, Northwestern University Feinberg School of Medicine, Chicago, Illinois 60611

ABSTRACT

Nuclear receptor subfamily 0, group B, member 1 (*Nr0b1;* hereafter referred to as *Dax1*) is an orphan nuclear receptor that regulates adrenal and gonadal development. Dosage-sensitive sex reversal, adrenal hypoplasia congenita, critical region on the X chromosome, gene 1 (*Dax1*) mutations in the mouse are sensitive to genetic background. In this report, a spectrum of impaired gonadal differentiation was observed as a result of crossing the *Dax1* knockout on the 129SvIm/J strain onto the C57BL/6J strain over two generations of breeding. *Dax1*-mutant XY mice of a mixed genetic background (129;B6*Dax1*$^{-/Y}$ [101 total]) developed gonads that were predominantly testislike (n = 61), ovarianlike (n = 27), or as intersex (n = 13). During embryonic development, *Sox9* expression in the gonads of 129;B6*Dax1*$^{-/Y}$ mutants was distributed across a wide quantitative range, and a threshold level of *Sox9* (>0.4-fold of wild-type) was associated with testis development. Germ cell fate also varied widely, with meiotic germ cells being more prevalent in the ovarianlike regions of embryonic gonads, but also observed within testicular tissue. *Ptgds,* a gene associated with *Sox9* expression and Sertoli cell development, was markedly downregulated in *Dax1*$^{-/Y}$ mice. *Stra8,* a gene associated with germ cell meiosis, was upregulated in *Dax1*$^{-/Y}$ mice. In both cases, the changes in gene expression also occurred in pure 129 mice but were amplified in the B6 genetic background. Sertoli cell apoptosis was prevalent in 129;B6*Dax1*$^{-/Y}$ gonads. In summary, *Dax1* deficiency on a partial B6 genetic background results in further modulation of gene expression changes that affect both Sertoli cell and germ cell fate, leading to a phenotypic spectrum of gonadal differentiation.

Dax1, *developmental biology, gamete biology, germ cell sex,* Nr0b1, *ovary, Sertoli cells, sex determination*

INTRODUCTION

The important cell fate decisions that direct early gonadal development center on the somatic cell population and the germ cell lineage. Pre-Sertoli cell commitment is critical for testis development, whereas meiotic entry signifies germ cell fate determination in the ovary. The bipotential gonad remains undifferentiated in the embryo until about midgestation in the mouse, after which point a genetic cascade establishes distinctly male or female sex characteristics by dictating somatic and germ line cell fates. Two male-determining genes, *Sry* and *Sox9*, have been identified for their molecular role in Sertoli cell determination and testis differentiation [1, 2]. Transgenic expression of either *Sry* or *Sox9* is sufficient to induce testis development in XX mice [3, 4]. Genetic studies in mice have also sought to elaborate the cellular and morphogenetic outcomes imposed by the network of genes involved in the mammalian sex determination cascade [5] and genetic disorders of reproduction [6].

Nuclear receptor subfamily 0, group B, member 1 (*Nr0b1*; hereafter referred to as *Dax1)* is an X-linked gene that acts at several levels of the reproductive axis. The 470-amino acid protein encoded by Dosage-sensitive sex reversal, adrenal hypoplasia congenita, critical region on the X chromosome, gene 1 (*Dax1*) belongs to the nuclear receptor superfamily [7]. *Dax1* is expressed in several endocrine organs, including the ventromedial hypothalamus, anterior pituitary, adrenal cortex, testis, and ovary [8]. In a mouse *Dax1* knockout model, male mice on the 129SvIm/J background (129*Dax1*$^{-/Y}$) were found to have testis abnormalities characterized by dilated seminiferous tubules and failed spermatogenesis [9]. The dilated tubules in the adult reflected impaired testis cord morphogenesis during embryonic development [10], resulting in the eventual obstruction of tubules and loss of germ cells [11]. Although the expression of Sertoli cell markers, such as *Sox9* and *Dhh*, was not significantly altered in the embryonic gonad of mice with a 129SvIm/J background, peritubular myoid cell number was reduced, possibly accounting for abnormal testis cord formation [10].

The role of *Dax1* in the male sex determination pathway was highlighted using the *Mus domesticus poschiavinus* mouse, an outbred strain with a "weakened" *Sry* allele (reduced and delayed mRNA expression of *Sry*) [12–14]. In the presence of the *Sry*^{Pos} allele, all genetically male *Dax1* mutant mice were sex reversed, even though the expression of *Sry* was not altered [15]. However, *Sox9* was not expressed, indicating that the molecular action of *Dax1* occurs downstream of *Sry* but before expression of *Sox9*. A similar phenomenon of sex reversal was observed when breeding the *Dax1* knockout allele from the originally reported 129SvIm/J background onto the C57BL/6J background (B6) [16]. On a congenic B6 background (obtained by continuous backcrosses), *Dax1* knockout mice fail to upregulate *Sox9*, even in the presence of full *Sry* expression from a *Mus musculus Sry* allele. In summary, *Dax1* loss of function in the mouse yields an XY gonadal phenotype that ranges from disordered testis cords in *M. musculus* 129SvIm/J to complete sex reversal in *M. domesticus poschiavinus* or congenic *M. musculus* C57BL/6J.

By taking advantage of the sensitizing effect of the B6 strain, the aim of the current study was to evaluate the intermediary phenotype of *Dax1* deficiency on gonadal and

[1]Supported by National Institutes of Health grant R01HD04481. S.Y.P. is a recipient of a Dolores Zohrab Liebmann Fellowship.
[2]Correspondence: J. Larry Jameson, Northwestern University Feinberg School of Medicine, Medical Dean's Administration, Morton 4-656, 303 E. Chicago Ave., Chicago, IL 60611. FAX: 312 503 7757; e-mail: ljameson@northwestern.edu
[3]Current address: Institut de Génétique et de Biologie Moléculaire et Cellulaire, 1 Rue Laurent Fries, B.P. 10142, 67404 Illkirch Cedex, France.

Received: 30 March 2008.
First decision: 18 April 2008.
Accepted: 30 June 2008.

ISSN: 0006-3363. http://www.biolreprod.org

TABLE 1. Phenotypic spectrum of reproductive defects associated with 129;B6*Dax1*$^{-/Y}$ animals.

Genotype	External sex	No. of animals	Internal genitalia	Features
XY;*Dax1*$^{-/Y}$	Male	61	Hypogonadal	Reduced testis weight combined with differentiation of epididymes, vas deferens, and seminal vesicles (as previously reported [9]).
XY;*Dax1*$^{-/Y}$	Male	9	Intersex	Marked by gonadal tissue having either ovarian or testicular features upon histological evaluation; female or male gonadal tissue were found to develop asymmetrically. Persistent Müllerian duct was a common feature.
Total		70		
XY;*Dax1*$^{-/Y}$	Female	4	Intersex	Gonads contained ovarian or testicular tissue. Duplex uterus developed with bilateral vestigial Wolffian ducts. Mixed tissue composed of epididymis and oviduct was observed by histology.
XY;*Dax1*$^{-/Y}$	Female	16	Dysgenesis	Gonadal tissue marked by undifferentiated cells resembling stromal tissue. Duplex uterus with varying degrees of Wolffian duct maturation.
XY;*Dax1*$^{-/Y}$	Female	11	Sex reversal	Ovaries with oocyte-containing follicles; oviduct and uterus development in the absence of male reproductive tissues.
Total		31		

sexual development. The goal was to understand which aspects of testis development are most sensitive to *Dax1* deficiency and are susceptible to the B6 genetic background.

MATERIALS AND METHODS

Genotyping and Assessment of Features of Sexual Differentiation

All procedures described within this article were reviewed and approved by the Northwestern University Institutional Animal Care and Use Committee, and they were performed in accordance with the Guiding Principles for the Care and Use of Laboratory Animals. Animals were killed by CO_2 inhalation at 12–16 wk of age. Genotyping for *Dax1* and *Sry* were performed on all progeny at the time of weaning. External genitalia were assessed by measurement of the anogenital distance. Dissection of internal genitalia was performed, and tissue was fixed in 10% neutral buffered formalin for routine histology. Processed tissue was embedded in paraffin, and 4-μm sections were stained with hematoxylin (Surgipath, Richmond, IL) and eosin (Fisher Scientific, Fair Lawn, NJ).

Quantitative Real-Time RT-PCR

Total RNA from individually dissected embryonic gonad-mesonephros complex pairs was extracted using Trizol (Invitrogen, Carlsbad, CA). Complementary DNA was synthesized using 200 ng RNA template combined with MMLV reverse transcriptase (Promega, Madison, WI), random primers (Roche Diagnostic, Nutley, NJ), and dinucleotide triphosphates (Promega) in a 20-μl reaction. Real-time RT-PCR product was measured by SYBR Green fluorescence emission using the Bio-Rad iCycler real-time system (Bio-Rad, Hercules, CA). A two-step cycling program (T_m of 55°C or 60°C) used 2 μl of the RT reaction containing cDNA. The threshold cycle number (C_t) was determined for each sample. Samples were tested in duplicate; at least six samples were tested for each genotype group. For each gene of interest, the averaged C_t value in both the reference group (ref) and the experimental group (exp) were normalized to the corresponding C_t value of the internal control gene, *RPL19* (ctl). The reference group refers to wild-type control. The relative expression was calculated based on the following equation: $2^{(\text{ref-ctl})}/2^{(\text{exp-ctl})}$. Values are reported as the average ± SD. Statistical significance was determined by performing an unpaired Student *t*-test analysis ($P < 0.05$). Primers used were (5′ to 3′): *Sox9*, forward: AAGAAAGACCACCCCGATTACA, reverse: CAGCGCCTTGAAGATAGCATT; *Ptgds*, forward: GCTCTTCGCATGCTGTGGAT, reverse: GCCCCAGGAACTTGTCTTGTT; *Stra8,* forward: TCGATCTCTCCCACTCCT, reverse: CAGAGACAATAGGAAGTGTC; and the internal control *RPL19* forward: CTGAAGGTCAAGGGAAATGTG, reverse: GGACAGAGTCTTGATGATCTC.

Whole-Mount In Situ Hybridization

A PCR-amplified cDNA fragment of the prostaglandin D2 synthase gene (NM_008963; nucleotides 343–723) was inserted into the pCMV-Sport6 plasmid vector (Invitrogen, Carlsbad, CA). Plasmids were linearized, and digoxygenin (DIG)-labeled riboprobes were generated by T7 RNA polymerase using a DIG RNA labeling mix (Roche, Nutley, NJ). Embryonic gonads were dissected at 13.5 days postcoitum (dpc). Following fixation and tissue processing, hybridization with DIG-labeled riboprobe occurred overnight. Bound probe was detected with an anti-DIG antibody labeled with alkaline phosphatase, followed by an NBT-BCIP enzyme substrate reaction (Roche), which yielded a purple color product where mRNA transcripts were present. A minimum of four gonads were tested for each genotype group.

Immunohistochemistry and Confocal Microscopy

Paraffin-embedded embryos were cut to 4-μm thickness to obtain tissue sections for immunostaining. Deparaffinized slides were subjected to antigen retrieval by high-temperature sodium citrate buffer prior to blocking and primary antibody incubation. GammaH2AX antibody (mouse host) was available through Upstate Cell Signaling (Charlottesville, VA), and the M.O.M. kit (mouse-on-mouse) from Vector Laboratories (Burlingame, CA) was used for detection. Goat anti-AMH antibody was purchased from Santa Cruz Biotechnologies (Santa Clara, CA). Alexa-conjugated secondary antibodies were obtained from Invitrogen. Confocal image microscopy was enabled by a Zeiss UV Laser Scanning Microscope 510 Meta (Thornwood, NY). Imaging was performed with Zeiss LSM software version 3.2.

Detection and Quantitation of Apoptotic Cells

Gonadal sections were processed for histochemical analysis as described above. The TUNEL assay kit was a product of Calbiochem (EMD Biosciences, San Diego, CA). Images were captured by confocal microscopy. A minimum of $n = 9$ embryos were evaluated in the 129;B6 *Dax1* mutant genotype group; $n = 4$ embryos were evaluated for each wild-type control group. The number of apoptotic cells was counted on individual tissue sections (at least four sections per individual embryo), then averaged for each genotype group.

RESULTS

Dax1 *Knockout Mice on a Mixed Genetic Background of 129SvIm/J and C57BL/6J Display a Phenotypic Spectrum of Sexual Differentiation*

Breeding of 129SvIm/J (129) *Dax1* knockout mice onto the C57BL/6J (B6) genetic background resulted in male-to-female sex reversal in as few as two generations of breeding (designated 129;B6). *Dax1* mutant animals (129;B6*Dax1*$^{-/Y}$) were grouped by external appearance as male or female without ambiguity (by the measurement of anogenital distance in mice). A total of 101 129;B6*Dax1*$^{-/Y}$ mutants were characterized out of 489 animals of the same breeding generation. The majority of 129;B6*Dax1*$^{-/Y}$ animals were male in appearance (70 of 101; Table 1). By contrast, 31 out of 101 129;B6*Dax1*$^{-/Y}$ animals were externally female. Examination of internal reproductive tissues in 101 mutant animals revealed a diverse spectrum of defects related to sex differentiation which are summarized in Table 1. Representative histology of the spectrum of phenotypes observed in 129;B6*Dax1*$^{-/Y}$ mutants is shown in Figure 1. As a reference,

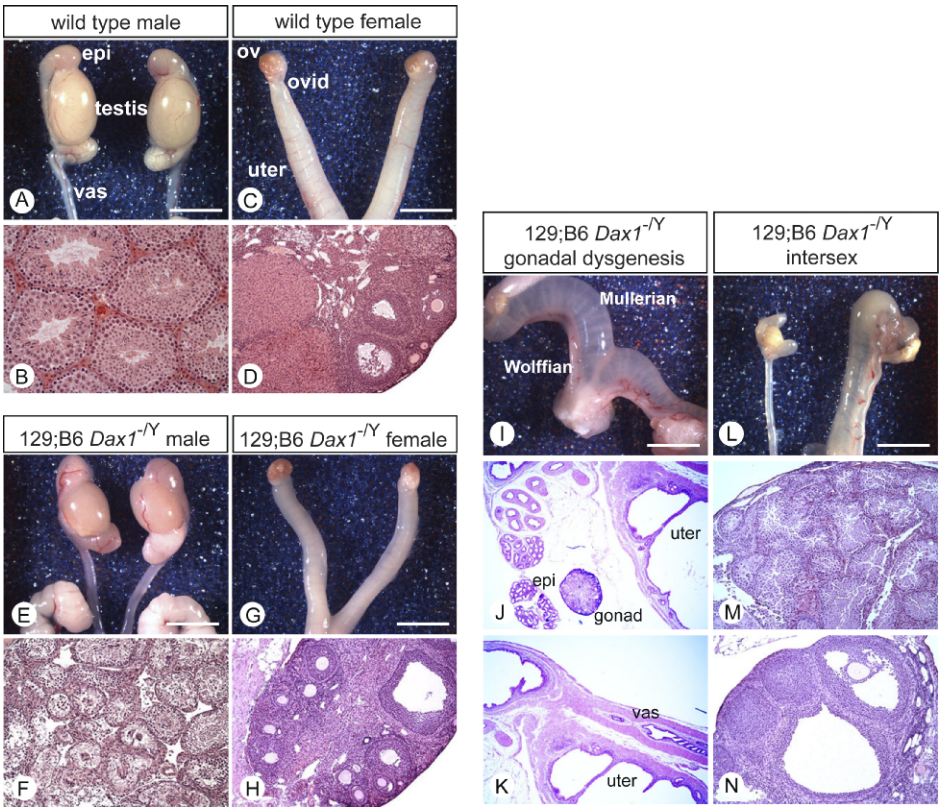

FIG. 1. Phenotypic spectrum of sexual development in 129;B6*Dax1*$^{-/Y}$ animals. Adult male and female internal genitalia of wild-type mice are shown for comparison to mutants (**A**–**D**). **A**) Wild-type males develop bilateral testis, epididymis (epi), and vas deferens (vas). **C**) Wild-type females have ovary (ov), oviduct (ovid), and uterus (uter). **B**, **D**) Cross-sectional histology of 12-wk-old testis (**B**) and ovary (**D**). In contrast, 129;B6*Dax1*$^{-/Y}$ animals (**E**–**N**) displayed a spectrum of reproductive defects from male hypogonadism to complete sex reversal. **E**) Those that developed externally as males had testes that were reduced in size, but otherwise these animals resembled the overall male phenotype. **F**) Representative histology of a *Dax1* mutant testis cross section. **G**) Complete sex reversal was evident in 129;B6*Dax1*$^{-/Y}$ animals that developed entirely with female reproductive tissue. **H**) In sex-reversed animals, oocyte-containing follicles were apparent by histology. **I**–**K**) Gonadal dysgenesis was a feature of certain sex-reversed mutant animals (gonad, **J**). Defects in duct development were evident, shown by the presence of bilateral uteri (uter, **K**) with vestigial Wolffian structures (epi, **J**; vas, **K**). **L**) An example of a 129;B6*Dax1*$^{-/Y}$ intersex mouse in which evidence for both testis formation (**M**) and ovarian development (**N**) was apparent in the same animal. Bars = 0.5 cm. Original magnification ×200 (**B**); ×100 (**D**, **F**, **H**); ×25 (**J**, **K**); ×100 (**M**, **N**).

gross anatomy and histology of wild-types of each sex are presented (Fig. 1, A–D). Dissection of *Dax1*-mutants at 12–16 wk of age revealed that the majority of external males were hypogonadal [61/70; Table 1] (testis weight approximately one third of wild-type) with normal testicular descent (Fig. 1, E and F). Epididymis, vas deferens and other secondary male structures developed normally. External females were also identified in the 129;B6*Dax1*$^{-/Y}$ genotype group, presenting a range of phenotypes from complete male-to-female sex reversal [11/31] (1G, H) to gonadal dysgenesis [16/31] (1I, J, K). Intersex mice (containing both male and female internal reproductive features- 1L, M, N) were also observed among 129;B6*Dax1*$^{-/Y}$ animals. Intersex mice could be either male or female in external appearance (9 male; 4 female; Table 1). Sex-reversed mice were infertile.

Quantitation of Sox9 *Expression in 129;B6*Dax1$^{-/Y}$ *Developing Gonads*

The molecular basis of sex reversal in 129;B6*Dax1*$^{-/Y}$ mice was examined by quantitative analysis of the male-determining gene *Sox9*. In previous studies, *Sox9* expression was detectable by in situ hybridization in 129*Dax1*$^{-/Y}$ gonads that developed (100%) as males, and was not significantly different from wild-type male gonads [10]. In contrast, *Sox9* expression was abrogated on a congenic B6 background, which conferred 100% sex reversal [16]. To determine whether *Sox9* levels correlate with gonadal sex in the *Dax1* mutant mice on a mixed background, *Sox9* expression was measured from mRNA taken from individual 129;B6*Dax1*$^{-/Y}$ mutant gonads isolated at 13.5 dpc (Fig. 2). Gonadal sex was designated at the time of dissection by the presence of embryonic testis cords and by gonad size, two distinguishing features of the male gonad [17]. In Figure 2, *Sox9* levels in wild-type male and female controls, respectively, are indicated by separately marked horizontal lines; wild-type males served as the reference group for *Sox9* quantitation. *Sox9* expression from a total of 31 gonads that were 129;B6*Dax1*$^{-/Y}$ were plotted individually. Overall, male development in 20 embryos (Fig. 2, individual dashes) was characterized by *Sox9* levels between approximately 0.4- and 1.0-fold of that in wild-type males (18 of 20 embryonic males). The *Sox9* levels in the majority of embryos with a female morphology (Fig. 2, triangles) were below 0.4-fold of wild-type males (8 of 11 embryonic females). In a few cases (3 of 11), female development occurred at levels of *Sox9* above 0.4-fold. These results suggest that *Dax1* deficiency on a partial B6 background results in a quantitative modulation of *Sox9* expression. Thus, a threshold level of *Sox9* mRNA may be required for testis differentiation.

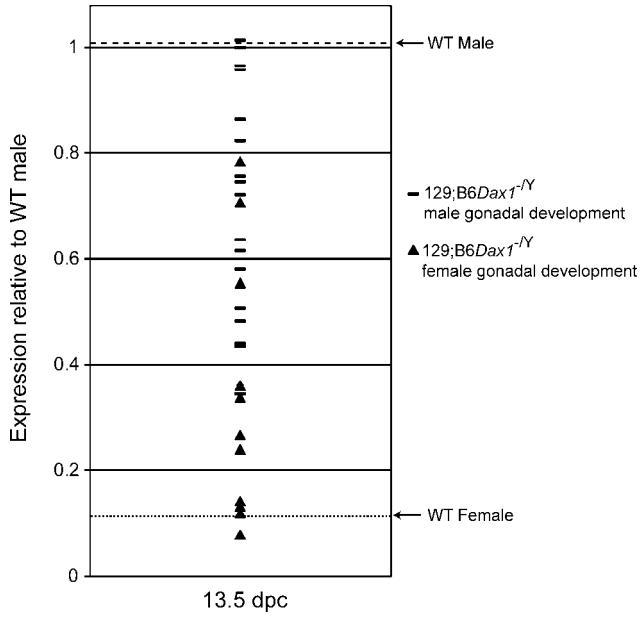

FIG. 2. *Sox9* expression in 129;B6*Dax1*$^{-/Y}$ gonads is modulated depending on genetic background. *Sox9* expression levels of gonad pairs from 31 embryos of 129;B6*Dax1*$^{-/Y}$ were calculated with reference to wild-type (WT) male (y-axis) then plotted individually. Quantitative real-time RT-PCR was performed on transcripts of gonad-mesonephros complexes dissected at Embryonic Day 13.5 dpc. Gonad sex was determined at the time of dissection (male, n = 20, individual dashes; female, n = 11, triangles). Expression levels of male and female controls are indicated by separate horizontal lines.

*Ectopic Entry of XY Male Germ Cells into Meiosis in 129;B6*Dax1$^{-/Y}$ *Gonads Varies in Pattern of Appearance*

The fate of embryonic germ cells in 129;B6*Dax1*$^{-/Y}$ animals was also addressed. During embryonic development, female germ cells undergo meiosis; in males, meiosis takes place after birth. Histone H2AFX (H2A Histone Family, member X, or H2AX) is rapidly phosphorylated at the sites of DNA double strand break that occur during meiotic crossover. The modified histone protein (gammaH2AX) is widely detected (Fig. 3) in the nuclei of germ cells of wild-type female gonad tissue at 14.5 dpc (Fig. 3A), and it is absent from wild-type male gonad tissue (Fig. 3F). Using an antibody directed against gamma-H2AX, meiotic germ cells were detected in mutant 129;B6*Dax1*$^{-/Y}$ gonads examined at 14.5 dpc (n = 12). The pattern of distribution of gammaH2AX-positive cells throughout the gonadal field varied considerably, and a summary of representative images of 129;B6*Dax1*$^{-/Y}$ gonads is shown (Fig. 3, B–E). Meiotic germ cells were present throughout the length of the gonad in some mutants, as seen in Figure 3, B and C, although more sparsely than in wild-type females. Some 129;B6*Dax1*$^{-/Y}$ gonads exhibiting meiotic germ cells developed with a male morphology (Fig. 3, D and E, compared with wild-type male). It should be noted that meiotic germ cells were never detected in 129*Dax1*$^{-/Y}$ gonads that are not susceptible to sex reversal (data not shown). In summary, meiotic entry in 129;B6*Dax1*$^{-/Y}$ gonads is nonuniform, suggesting local interactions between somatic and germ cell microenvironments.

Ptgds *Expression Is Decreased in* Dax1 *Knockout Gonads*

To examine the molecular consequences associated with the modulation of *Sox9* expression and the ectopic entry of germ cells into meiosis, the expression of prostaglandin D2 synthase (*Ptgds*) was compared among *Dax1* mutants of different genetic backgrounds. *Ptgds* is the rate-limiting enzyme in prostaglandin D2 production, and it is a member of the lipocalin family of retinoid transport proteins. Its expression is sexually dimorphic, and in the testis it is linked to *Sox9* induction [18]. Whole-mount in situ hybridization was performed on gonads at 13.5 dpc (Fig. 4). *Ptgds* expression

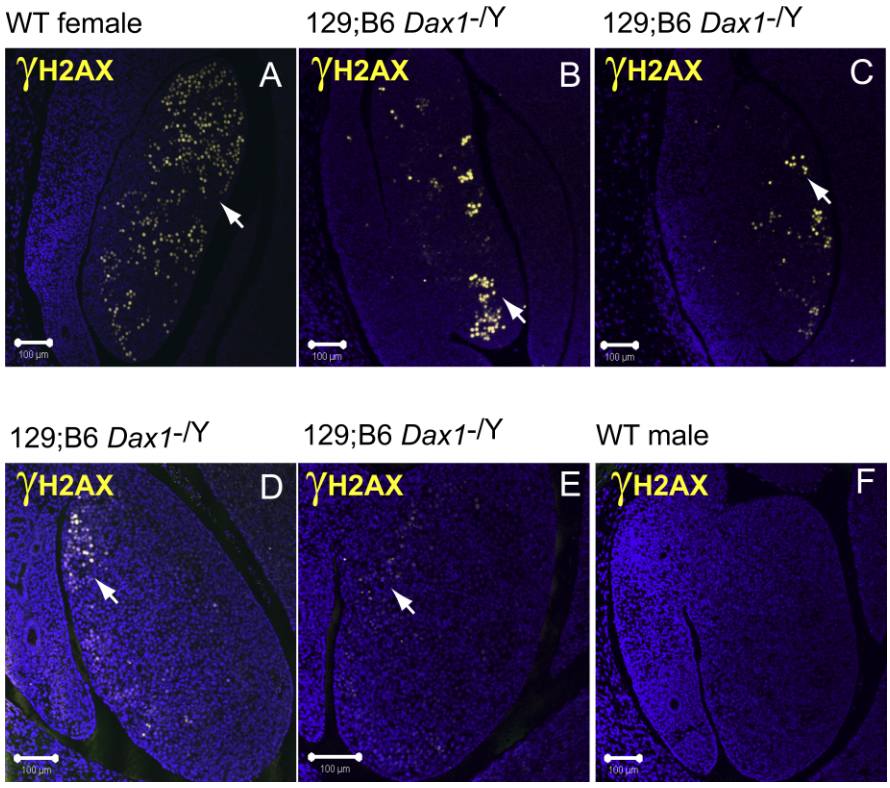

FIG. 3. Distribution pattern of ectopic meiotic germ cells in gonads susceptible to sex reversal. To investigate PGC fate in gonads of 129;B6*Dax1*$^{-/Y}$ animals, germ cell sex was examined by immunodetection of gammaH2AX, a marker of phosphorylated histones that signifies meiotic entry. **A**) Female PGCs commence meiosis during embryonic development, and by 14.5 dpc meiotic germ cells are detected along the length of the gonad (arrow). **B**–**E**) A representative spectrum of 129;B6*Dax1*$^{-/Y}$ gonadal tissue demonstrates the variable manner in which meiotic germ cells appear during development. Micrographs **B** and **C** show two examples of *Dax1* mutant gonad tissue resembling female development that contained gammaH2AX-positive germ cells dispersed in clusters along the gonad length (arrows), whereas **D** and **E** revealed meiotic germ cells (arrows) located in tissue with testislike morphology. In wild-type male gonads (**F**), meiotic germ cells were characteristically undetectable. Bar = 100 μm.

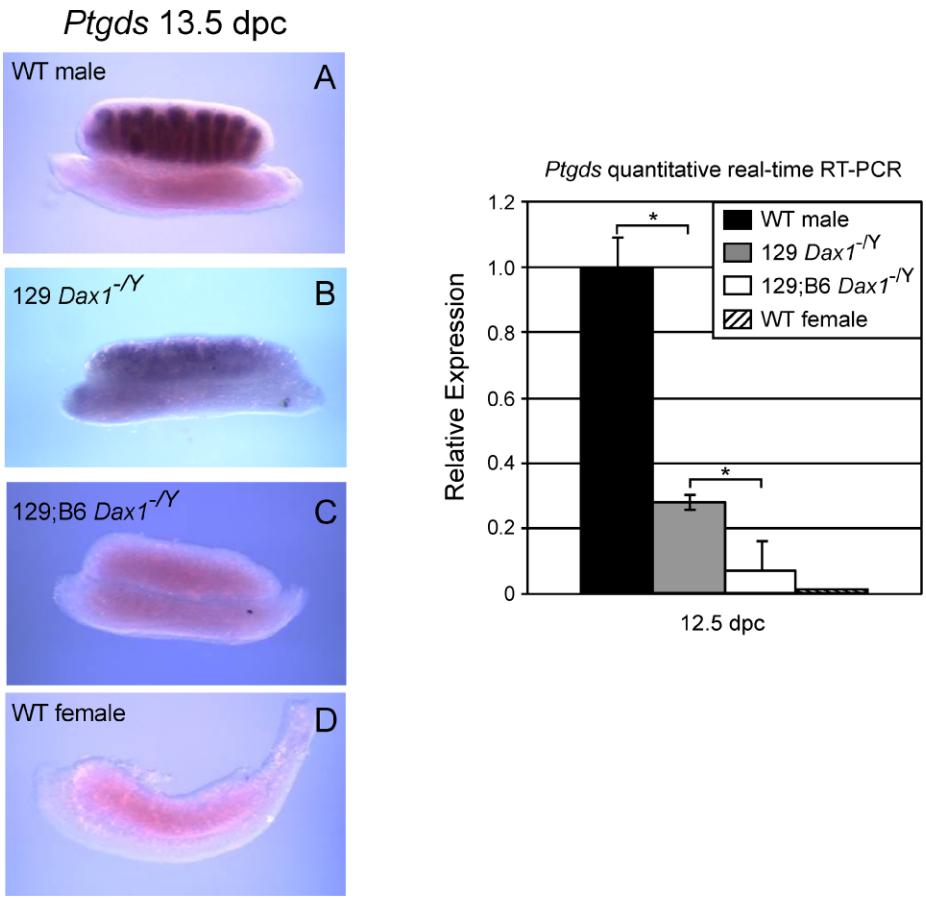

FIG. 4. Embryonic gonadal expression of *Ptgds* is dependent on *Dax1*. In situ hybridization of *Ptgds* on whole-mount gonads at 13.5 dpc was performed on wild-type male gonads (**A**), in which expression is detected in testis cords. *Ptgds* expression was less distinct in 129*Dax1*$^{-/Y}$ gonads (**B**), and it was further abolished in 129;B6*Dax1*$^{-/Y}$ gonads (**C**) of mixed background. As a negative control (**D**), wild-type females had no detectable *Ptgds* expression. Quantitative expression levels of *Ptgds* transcripts were measured in embryonic gonads at 12.5 dpc by real-time RT-PCR (graph). In each case, relative expression (y-axis) was calculated with reference to wild-type (WT) male. There was a sexually dimorphic pattern of expression (compare WT male [black bar] vs. female [diagonally striped bar]). In 129*Dax1*$^{-/Y}$ gonads (gray bar), *Ptgds* transcript levels were markedly reduced, even though these mice mature as hypogonadal males. In 129;B6*Dax1*$^{-/Y}$ gonads (white bar) there was a further decrease in the expression levels of *Ptgds*. Bars represent mean ± SD. Statistical significance between genotype groups was evaluted by Student *t*-test; the asterisk symbol indicates a P value < 0.05.

was detected in wild-type male gonads (Fig. 4A) along embryonic testis cords, a pattern consistent with published data [19]. Expression was weaker and less distinctive in 129*Dax1*$^{-/Y}$ gonads (Fig. 4B). Furthermore, in 129;B6*Dax1*$^{-/Y}$ gonads (Fig. 4C), as in the female (Fig. 4D), there was no detectable expression by in situ hybridization (n = 4 per group). Additionally, *Ptgds* expression was quantitated by real-time RT-PCR in gonads dissected from 129 *Dax1*$^{-/Y}$ (not susceptible to sex reversal) and 129;B6 *Dax1*$^{-/Y}$ (susceptible to sex reversal) animals (Fig. 4, graph). Wild-type male expression levels served as the reference control (n = 6; Fig. 4, black bar in graph). In agreement with the results of in situ hybridization experiments, *Ptgds* expression was significantly reduced in 129 *Dax1*$^{-/Y}$ gonads, even without the influence of the B6 genetic background (n = 11; Fig. 4, gray bar in graph). A further reduction was apparent in 129;B6 *Dax1*$^{-/Y}$ gonads (n = 14; Fig. 4, white bar in graph), the levels of which were similar to that in female gonads (n = 15; Fig. 4, diagonally striped bar in graph). Because *Ptgds* expression was already attenuated in mutants on the pure 129 strain, this may explain why there was not a spectrum of expression in 129;B6 *Dax1*$^{-/Y}$ gonads. In summary, both in situ hybridization studies and quantitative real-time PCR demonstrate that *Ptgds* expression is attenuated in the absence of *Dax1*, and this reduction occurs regardless of genetic background.

Dax1 *Mutant Testes Exhibit Enhanced Expression of* Stra8

Prior to meiosis, local retinoic acid (RA) accumulation induces expression of *Stra8* (stimulated by RA) in primordial germ cells (PGCs) [20]. Since ectopic meiotic entry of germ cells was observed in 129;B6*Dax1*$^{-/Y}$ gonads, it was feasible that *Dax1* mutant gonads expressed inappropriate levels of *Stra8*. The expression levels of *Stra8* were measured in 129*Dax1*$^{-/Y}$ and 129;B6*Dax1*$^{-/Y}$ gonads (Fig. 5) at 13.0 and 14.5 dpc, the time in embryonic development when *Stra8* expression is initiated in the female gonad (n = 12; Fig. 5, white bars, relative control group) [21]. Whereas *Stra8* transcripts were not detected in wild-type males (n = 6; Fig. 5, diagonally striped bars), nor were they detected to a significant extent in 129*Dax1*$^{-/Y}$ gonads (n = 6; Fig. 5, gray bars), surprisingly, *Stra8* expression was upregulated as early as 13.0 dpc in 129;B6*Dax1*$^{-/Y}$ gonads (n = 7; Fig. 5, black bars). Thereafter, by 14.5 dpc, 129*Dax1*$^{-/Y}$ gonad *Stra8* levels (n = 6) reached nearly the same level as those in wild-type females (n = 10), whereas the level in 129;B6*Dax1*$^{-/Y}$ gonads (n = 6) exceeded that of the females. Therefore, upregulation of *Stra8* occurs in *Dax1* mutants and is further augmented on the B6 background.

*Sertoli Cells Undergo Apoptosis in 129;B6*Dax1$^{-/Y}$ *Gonads*

Histologic observation of cellular morphology in 129;B6*Dax1*$^{-/Y}$ gonads that were susceptible to sex reversal indicated that apoptosis was prevalent in the gonad. To clarify which cell types were undergoing programmed cell death, double immunostaining with the Sertoli marker, anti-Müllerian hormone (AMH; red), and the germ cell marker, phosphorylated histone H2AX (gammaH2AX; yellow), combined with TUNEL labeling (green) of apoptotic cells was undertaken (Fig. 6). Anti-Müllerian hormone was localized to the cytoplasm of Sertoli cells located in the wild-type male gonad (Fig. 6A, within the testis cords) and also in 129;B6*Dax1*$^{-/Y}$ gonads (Fig. 6B). In wild-type females AMH was characteristically absent (Fig. 6C). Labeling of AMH along with TUNEL detection in gonad tissue

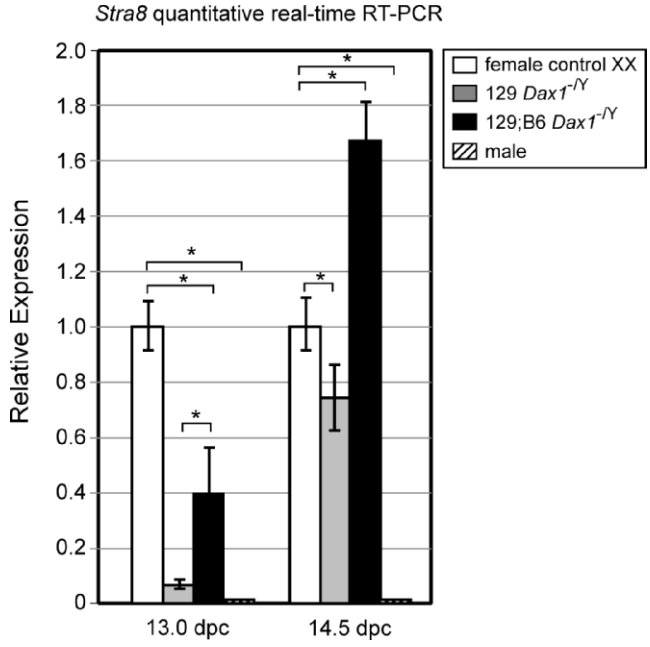

FIG. 5. Upregulation of *Stra8* expression level in PGCs of *Dax1* mutant gonads. *Stra8* expression was measured to assess the commitment steps of the PGC lineage in *Dax1*-mutant gonads on both the pure 129 and the mixed 129;B6 backgrounds. Since *Stra8* is a female-specific gene, the relative expression (y-axis) was measured with reference to wild-type female (white bars). *Stra8* expression is sexually dimorphic during development; thus, males lack detectable levels of expression (diagonally striped bars). Quantitative real-time RT-PCR was performed at two timepoints: 13.0 and 14.5 dpc. In 129*Dax1*$^{-/Y}$ gonads, which develop as males, the level of *Stra8* expression at 13.0 dpc (gray bars) was low, then increased significantly by 14.5 dpc, to reach a level nearly as high as the one in females. In 129;B6*Dax1*$^{-/Y}$ gonads (black bars), in which sex reversal was observed, *Stra8* transcript abundance was markedly increased as early as 13.0 dpc, then exceeded female levels by 14.5 dpc. Bars represent mean ± SD. Statistical significance between genotype groups was evaluted by Student *t*-test; the asterisk symbol indicates a *P* value < 0.05.

sections showed that apoptosis was prevalent in the Sertoli cells of 129;B6*Dax1*$^{-/Y}$ gonads (Fig. 6B). Cell death was not observed in wild-type male or female gonadal tissue. For the wild-type male and female groups, n = 4 animals were tested; for the 129;B6*Dax1*$^{-/Y}$ group, n = 9 animals were tested. All mutant gonads tested exhibited Sertoli cell apoptosis. On average, 129;B6*Dax1*$^{-/Y}$ gonads contained approximately 87 ± 28 TUNEL-positive cells per gonadal field (Fig. 6, graph). Nuclei were stained with 4′,6′-diamidino-2-phenylindole (blue) on all sections. Notably, TUNEL-positive Sertoli cells were not detected in the pure background 129*Dax1*$^{-/Y}$ gonads (data not shown).

In addition, double immunostaining to detect gamma-H2AX-positive germ cells (yellow) and apoptotic cells (green) did not overlap in 129;B6*Dax1*$^{-/Y}$ mutants (Fig. 6E), indicating that the germ cell population was not the major cell type undergoing apoptosis. Wild-type male and female served as negative and positive controls, respectively, for gammaH2AX staining (Fig. 6, D and F). These data indicate an essential role for *Dax1* in combination with B6 alleles in Sertoli cell survival.

DISCUSSION

Humans carrying genetic mutations in *DAX1* are characterized by defects in adrenal function and aberrant gonadal differentiation [22]. To begin to understand the basic mechanisms underlying the origins of gonadal defects associated with *DAX1* mutation, a model of *Dax1* loss of function was used in which a change in the genetic background augmented the phenotype from male hypogonadism to complete male-to-female sex reversal. By examining the intermediary phenotype of *Dax1* mutants on a 129;B6 background, we have shown that *Dax1* plays an important role in Sertoli cell differentiation and survival in the bipotential gonad. *Dax1* promotes the male pathway through modulation of *Sox9* expression (directly or indirectly), a factor that is known to be required for Sertoli cell differentiation [23, 24]. In the absence of *Dax1*, *Sox9* expression is sensitive to the B6 genetic background, as revealed by reduced (as shown in this work) or abrogated [16] expression. Of note, *Sox9* was also markedly reduced in the *M. domesticus poschiavinus* strain in the absence of *Dax1* [15]. Although these findings were initially attributed to a weakened *Sry* allele characteristic of the *poschiavinus* strain, it is also plausible that autosomal genes, such as the chromosome 4 gene *tda1*, contributed to sex reversal in the absence of *Dax1* [25].

Here, *Dax1* deficiency was shown to result in Sertoli cell apoptosis in developing gonads that were susceptible to sex reversal by the influence of the B6 background. It is not clear whether apoptosis was cell autonomous in the Sertoli lineage due to the loss of *Dax1* or, if in combination with modifying factors, paracrine cell-cell signals triggered an apoptotic cascade. The milieu of meiotic germ cells might also have contributed to apoptosis in Sertoli cells of 129;B6*Dax1*$^{-/Y}$ gonads.

Ptgds was shown to require *Dax1* for its full expression, since it was significantly downregulated in 129 pure background mutants. Its role in the testis may explain some of the phenotypic features associated with sex reversal in 129;B6*Dax1*$^{-/Y}$ gonads. For example, it has been shown that dimeric Sox9 binds to the *Ptgds* promoter [26]. Moreover, exogenous prostaglandin D2 addition to XX gonad explants in culture can induce ectopic *Sox9* expression [18]. Thus, a feed-forward loop is thought to exist between *Sox9* and *Ptgds*. Whether *Dax1* plays a role in this feed-forward loop requires further investigation.

Interestingly, *Stra8* expression was upregulated in both 129*Dax1*$^{-/Y}$ gonads (male development) and in 129;B6*Dax1*$^{-/Y}$ gonads (exhibiting sex reversal), suggesting the possibility that *Dax1* is a repressor of factors controlling *Stra8* expression. The *Stra8* gene is expressed in embryonic germ cells of female gonads [21] in response to the presence of local RA. Retinoic acid plays an important regulatory role in the control of germ cell meiotic entry [20]. One explanation for this consistent upregulation of *Stra8* in *Dax1* mutants regardless of genetic background is impaired peritubular myoid development [10]. Peritubular myoid cells and the basal lamina may provide a physical barrier that prevents RA diffusion into the compartment of testis cords, thus protecting male germ cells from RA exposure. Additionally, it is thought that RA exposure is circumvented in the male gonad by the presence of CYP26B1 [27], an RA-degrading enzyme expressed in Sertoli cells during development [28] and in adult peritubular myoid cells [29]. On the 129 genetic background, *Cyp26b1* mRNA levels (12.5 and 13.5 dpc) were not statistically different in *Dax1* mutants and wild-type males (data not shown). Therefore, a reduction in *Cyp26b1* alone does not account for the measured increase in *Stra8* on the 129 background. In congenic B6 *Dax1*$^{-/Y}$ mice, the level of *Cyp26b1* expression was reduced to that of females [16]. Further developmental studies of *Cyp26b1* expression in different cell types will be of interest to illuminate the pathways

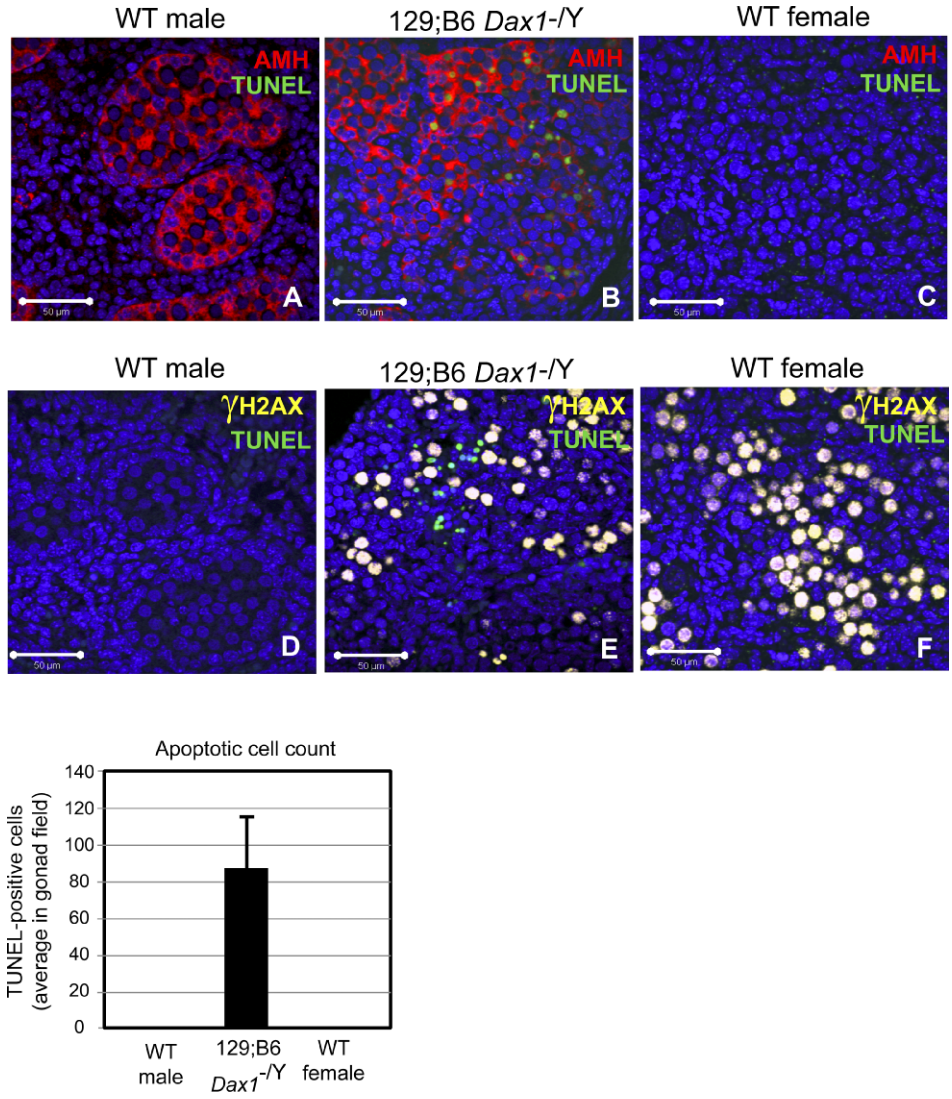

FIG. 6. Loss of *Dax1* leads to Sertoli cell apoptosis. Apoptotic cells were identified in the developing gonads of 129;B6*Dax1*$^{-/Y}$ mice. Double staining of either AMH (red) and TUNEL labeling (green), or gamma-H2AX (yellow) and TUNEL labeling revealed that apoptotic cells were of the Sertoli lineage. **A**) Cytoplasmic Sertoli cell staining of AMH in wild-type (WT) males demarcated testis cords, whereas TUNEL-positive cells were absent. **B**) A representative image of a 129;B6*Dax1*$^{-/Y}$ gonad section shows double staining of apoptotic cells with AMH-positive Sertoli cells (arrow). **C**) Wild-type female tissue lacked both AMH protein and apoptotic cells. **D**–**F**) Double labeling of gammaH2AX, a germ cell marker, combined with TUNEL detection was used to distinguish apoptotic germ cells. **D**) Males lacked gammaH2AX positivity, as expected. **E**) In 129;B6*Dax1*$^{-/Y}$ gonads, apoptotic nuclei did not overlap with staining for gammaH2AX (arrow). **F**) Females had characteristically high levels of gammaH2AX-containing cells. Once again, both wild-type control tissues lacked apoptotic cells. The average number of apoptotic cells per gonad field is represented in the graph. Error bar represents mean ± SD. Bar = 50 μm.

that govern differential germ cell development in the testis and ovary.

It should be emphasized that not all the defects observed in *Dax1* mutant gonads presented herein can be attributed to the B6 strain. As previously noted, both *Ptgds* and *Stra8* were strikingly deregulated in pure 129 mutants. On the other hand, *Dax1* mutant gonads on a pure 129 background showed no evidence of Sertoli cell apoptosis or germ cell meiosis. Thus, the B6 background affects the control of gene expression levels in different cell types during gonadal development. In summary, these studies of *Dax1* mutants on a mixed genetic background provide insights into the pathways governing cell fate decisions that determine gonadal sex. The first critical factor in male determination is *Sry*, followed by *Sox9*, both key elements in Sertoli cell fate determination. *Sox9* levels are subject to modulation, and a threshold level appears to be important for the male pathway to proceed. This suggests that *Sox9* dosage may be a critical determinant of somatic cell fate, as modulation of *Sox9* expression levels on the B6 background correlates with a male versus female gonadal fate. In parallel, germ cell meiosis during development hinges on the absence or downregulation of these male factors. Thus, in the bipotential gonad, the male and female pathways coexist until a developmental "tipping point" is quickly established [30]. Indeed, if a distinct fate choice is not enforced during development—as in the case of *Dax1* mutants of a mixed 129;B6 background—a spectrum of phenotypic combinations bearing both male and female features can develop. These features underscore the likelihood that many sex-determining genes function in a dosage-sensitive manner [31] and that genetic background influences the quantitative expression of these genes. Moreover, gonadal architecture, such as the formation of testis cords, is important to support Sertoli cell maturation in order to create niches for germ cells [32].

ACKNOWLEDGMENTS

Imaging and microscopy expertise was provided by Dr. Teong-Leong Chew, Dr. Paul Cheresh, and Lennell Reynolds of the Northwestern University Cell Imaging Facility. The authors wish to thank Dr. So-Youn Kim of the Jameson Laboratory for indispensable aid.

REFERENCES

1. Koopman P, Munsterberg A, Capel B, Vivian N, Lovell-Badge R. Expression of a candidate sex-determining gene during mouse testis differentiation. Nature 1990; 348:450–452.
2. Kent J, Wheatley SC, Andrews JE, Sinclair AH, Koopman P. A male-specific role for SOX9 in vertebrate sex determination. Development 1996; 122:2813–2822.

3. Koopman P, Gubbay J, Vivian N, Goodfellow P, Lovell-Badge R. Male development of chromosomally female mice transgenic for Sry. Nature 1991; 351:117–121.
4. Morais da Silva S, Hacker A, Harley V, Goodfellow P, Swain A, Lovell-Badge R. Sox9 expression during gonadal development implies a conserved role for the gene in testis differentiation in mammals and birds. Nat Genet 1996; 14:62–68.
5. Brennan J, Capel B. One tissue, two fates: molecular genetic events that underlie testis versus ovary development. Nat Rev Genet 2004; 5:509–521.
6. Wilhelm D, Koopman P. The makings of maleness: towards an integrated view of male sexual development. Nat Rev Genet 2006; 7:620–631.
7. Zanaria E, Muscatelli F, Bardoni B, Strom TM, Guioli S, Guo W, Lalli E, Moser C, Walker AP, McCabe ER, Meitinger T, Monaco AP, et al. An unusual member of the nuclear hormone receptor superfamily responsible for X-linked adrenal hypoplasia congenita. Nature 1994; 372:635–641.
8. Ikeda Y, Swain A, Weber TJ, Hentges KE, Zanaria E, Lalli E, Tamai KT, Sassone-Corsi P, Lovell-Badge R, Camerino G, Parker KL. Steroidogenic factor 1 and Dax-1 colocalize in multiple cell lineages: potential links in endocrine development. Mol Endocrinol 1996; 10:1261–1272.
9. Yu RN, Ito M, Saunders TL, Camper SA, Jameson JL. Role of Ahch in gonadal development and gametogenesis. Nat Genet 1998; 20:353–357.
10. Meeks JJ, Crawford SE, Russell TA, Morohashi KI, Weiss J, Jameson JL. Dax1 regulates testis cord organization during gonadal differentiation. Development 2003; 130:1029–1036.
11. Jeffs B, Meeks JJ, Ito M, Martinson FA, Matzuk MM, Jameson JL, Russell LD. Blockage of the rete testis and efferent ductules by ectopic Sertoli and Leydig cells causes infertility in Dax1-deficient male mice. Endocrinology 2001; 142:4486–4495.
12. Nagamine CM, Morohashi K, Carlisle C, Chang DK. Sex reversal caused by Mus musculus domesticus Y chromosomes linked to variant expression of the testis-determining gene Sry. Dev Biol 1999; 216:182–194.
13. Albrecht KH, Young M, Washburn LL, Eicher EM. Sry expression level and protein isoform differences play a role in abnormal testis development in C57BL/6J mice carrying certain Sry alleles. Genetics 2003; 164:277–288.
14. Palmer SJ, Burgoyne PS. The *Mus musculus domesticus* Tdy allele acts later than the Mus musculus musculus Tdy allele: a basis for XY sex-reversal in C57BL/6-YPOS mice. Development 1991; 113:709–714.
15. Meeks JJ, Weiss J, Jameson JL. Dax1 is required for testis determination. Nat Genet 2003; 34:32–33.
16. Bouma GJ, Albrecht KH, Washburn LL, Recknagel AK, Churchill GA, Eicher EM. Gonadal sex reversal in mutant Dax1 XY mice: a failure to upregulate Sox9 in pre-Sertoli cells. Development 2005; 132:3045–3054.
17. Schmahl J, Eicher EM, Washburn LL, Capel B. Sry induces cell proliferation in the mouse gonad. Development 2000; 127:65–73.
18. Wilhelm D, Martinson F, Bradford S, Wilson MJ, Combes AN, Beverdam A, Bowles J, Mizusaki H, Koopman P. Sertoli cell differentiation is induced both cell-autonomously and through prostaglandin signaling during mammalian sex determination. Dev Biol 2005; 287:111–124.
19. Adams IR, McLaren A. Sexually dimorphic development of mouse primordial germ cells: switching from oogenesis to spermatogenesis. Development 2002; 129:1155–1164.
20. Koubova J, Menke DB, Zhou Q, Capel B, Griswold MD, Page DC. Retinoic acid regulates sex-specific timing of meiotic initiation in mice. Proc Natl Acad Sci U S A 2006; 103:2474–2479.
21. Menke DB, Koubova J, Page DC. Sexual differentiation of germ cells in XX mouse gonads occurs in an anterior-to-posterior wave. Dev Biol 2003; 262:303–312.
22. Muscatelli F, Strom TM, Walker AP, Zanaria E, Recan D, Meindl A, Bardoni B, Guioli S, Zehetner G, Rabl W, Schwarz HP, Kaplan JC, et al. Mutations in the DAX-1 gene give rise to both X-linked adrenal hypoplasia congenita and hypogonadotropic hypogonadism. Nature 1994; 372:672–676.
23. Barrionuevo F, Bagheri-Fam S, Klattig J, Kist R, Taketo MM, Englert C, Scherer G. Homozygous inactivation of Sox9 causes complete XY sex reversal in mice. Biol Reprod 2006; 74:195–201.
24. Chaboissier MC, Kobayashi A, Vidal VI, Lutzkendorf S, van de Kant HJ, Wegner M, de Rooij DG, Behringer RR, Schedl A. Functional analysis of Sox8 and Sox9 during sex determination in the mouse. Development 2004; 131:1891–1901.
25. Eicher EM, Washburn LL, Schork NJ, Lee BK, Shown EP, Xu X, Dredge RD, Pringle MJ, Page DC. Sex-determining genes on mouse autosomes identified by linkage analysis of C57BL/6J-YPOS sex reversal. Nat Genet 1996; 14:206–209.
26. Wilhelm D, Hiramatsu R, Mizusaki H, Widjaja L, Combes AN, Kanai Y, Koopman P. SOX9 regulates prostaglandin D synthase gene transcription in vivo to ensure testis development. J Biol Chem 2007; 282:10553–10560.
27. Bowles J, Knight D, Smith C, Wilhelm D, Richman J, Mamiya S, Yashiro K, Chawengsaksophak K, Wilson MJ, Rossant J, Hamada H, Koopman P. Retinoid signaling determines germ cell fate in mice. Science 2006; 312:596–600.
28. Maclean G, Li H, Metzger D, Chambon P, Petkovich M. Apoptotic extinction of germ cells in testes of Cyp26b1 knockout mice. Endocrinology 2007; 148:4560–4567.
29. Vernet N, Dennefeld C, Rochette-Egly C, Oulad-Abdelghani M, Chambon P, Ghyselinck NB, Mark M. Retinoic acid metabolism and signaling pathways in the adult and developing mouse testis. Endocrinology 2006; 147:96–110.
30. Dinapoli L, Capel B. SRY and the standoff in sex determination. Mol Endocrinol 2008; 22:1–9.
31. Kim Y, Capel B. Balancing the bipotential gonad between alternative organ fates: a new perspective on an old problem. Dev Dyn 2006; 235:2292–2300.
32. Gassei K, Schlatt S. Testicular morphogenesis: comparison of in vivo and in vitro models to study male gonadal development. Ann N Y Acad Sci 2007; 1120:152–167.